# TNF-mediated survival of CD169+ cells promotes immune activation during vesicular stomatitis virus infection

Shinde, Prashant V.; Xu, Haifeng C.; Maney, Sathish Kumar; Kloetgen, Andreas; Namineni, Sukumar; Zhuang, Yuan; Honke, Nadine; Shaabani, Namir; Bellora, Nicolas; Doerrenberg, Mareike; Trilling, Mirko; Pozdeev, Vitaly I.; van Rooijen, Nico; Scheu, Stefanie; Pfeffer, Klaus; Crocker, Paul R.; Tanaka, Masato; Duggimpudi, Sujitha; Knolle, Percy; Heikenwalder, Mathias; Ruland, Jürgen; Mak, Tak W.; Brenner, Dirk; Pandyra, Aleksandra A.; Hoell, Jessica I.; Borkhardt, Arndt; Häussinger, Dieter; Lang, Karl S.; Lang, Philipp A.

*Published in:*
Journal of Virology

*DOI:*
10.1128/JVI.01637-17

*Publication date:*
2017

*Document Version*
Peer reviewed version

# Title: TNF-mediated survival of CD169$^{+}$ cells promotes immune activation during vesicular stomatitis virus infection

Prashant V. Shinde[1,2], Haifeng C. Xu[1,2], Sathish Kumar Maney[1,2], Andreas Kloetgen[3,4], Sukumar Namineni[5,13], Yuan Zhuang[1,2], Nadine Honke[6], Namir Shaabani[7], Nicolas Bellora[8], Mareike Doerrenberg[3], Mirko Trilling[9], Vitaly I. Pozdeev[1,2], Nico van Rooijen[10], Stefanie Scheu[11], Klaus Pfeffer[11], Paul R. Crocker[12], Masato Tanaka[13] Sujitha Duggimpudi[3], Percy Knolle[14], Mathias Heikenwalder[5,15], Jürgen Ruland[16], Tak W. Mak[17], Dirk Brenner[18,19], Aleksandra A. Pandyra[6], Jessica I. Hoell[3], Arndt Borkhardt[3], Dieter Häussinger[2], Karl S. Lang[6,+], and Philipp A. Lang[1,+,*]

[1]Department of Molecular Medicine II, Medical Faculty, Heinrich Heine University, Universitätsstr. 1, 40225 Düsseldorf, Germany, [2]Department of Gastroenterology, Hepatology, and Infectious Diseases, Heinrich-Heine-University Düsseldorf, Universitätsstr. 1, 40225 Düsseldorf, Germany, [3]Department of Pediatric Oncology, Hematology and Clinical Immunology, Center for Child and Adolescent Health, Heinrich Heine University, Medical Faculty, Duesseldorf, Germany, [4]Computational Biology of Infection Research, Helmholtz Center for Infection Research, Braunschweig, Germany, [5]Institute of Virology, TU Munich, Schneckenburgerstr. 8, 81675 München, Germany, [6]Institute of Immunology, Medical Faculty, University of Duisburg-Essen, Hufelandstr. 55, Essen 45147, Germany, [7]Department of Immunology and Microbial Science, The Scripps Research Institute, La Jolla, CA 92037, USA, [8]Instituto Andino Patagónico de Tecnologías Biológicas y Geoambientales (IPATEC), Universidad Nacional del Comahue - CONICET, Bariloche, Argentina, [9]Institute for Virology, University of Duisburg-Essen, Hufelandstr. 55, Essen 45147, Germany, [10]Department of Cell Biology, Vrije University Medical Center, 1081 BT Amsterdam, Netherlands, [11]Institute of Medical Microbiology and Hospital Hygiene, Heinrich-Heine-University Duesseldorf, 40225 Duesseldorf, Germany, [12]Division of Cell Signalling and Immunology, School of Life Sciences, University of Dundee, Dundee DD1 5EH, United Kingdom, [13]Laboratory of Immune regulation, School of Life Science, Tokyo University of Pharmacy and Life Sciences, 1432-1 Horinouchi, Hachioji, Tokyo 192-0392, Japan. [14]Institute of Molecular Immunology, Technische Universität München and Helmholtz Zentrum München, Munich, Germany, [15]Division of Chronic Inflammation and Cancer, German Cancer Research Center (DKFZ), Heidelberg, Germany, [16]Institut für Klinische Chemie und Pathobiochemie, Klinikum rechts der Isar, Technische Universität München, Munich, Germany, [17]Princess Margaret Cancer Center, University Health Network, Toronto, Ontario, Canada M5G 2C1, [18]Department of Infection and Immunity, Experimental and Molecular Immunology, Luxembourg Institute of Health, L-4354 Esch-sur-Alzette, Luxembourg, [19]Odense Research Center for Anaphylaxis (ORCA), Department of Dermatology and Allergy Center, Odense University Hospital, University of Southern Denmark, Odense, Denmark;

*Address correspondence to PAL: langp@uni-duesseldorf.de

+ contributed equally to this work

Key words: TNF, MALT1, innate immunity, interferon, NF-κB

## Abstract

Innate immune activation is essential to mount an effective antiviral response and to prime adaptive immunity. Although a crucial role of $CD169^+$ cells during vesicular stomatitis virus (VSV) infections is increasingly recognized, factors regulating $CD169^+$ cells during viral infections remain unclear. Here we show that tumor necrosis factor is produced by $CD11b^+$ $Ly6C^+Ly6G^+$ cells following infection with VSV. The absence of TNF or TNF receptor 1 (TNFR1) resulted in reduced numbers of $CD169^+$ cells and in reduced IFN-I production during VSV infection, with a severe disease outcome. Specifically, TNF triggered RelA translocation into the nucleus of $CD169^+$ cells; this translocation was inhibited when paracaspase MALT-1 was absent. Consequently, MALT1 deficiency resulted in reduced VSV replication, defective innate immune activation, and severe disease development. These findings indicate that TNF mediates the maintenance of $CD169^+$ cells and innate and adaptive immune activation during VSV infection.

## Importance

Over the last decade, strategically placed $CD169^+$ metallophilic macrophages in the marginal zone of the murine spleen and LN have been shown to play a very important role in host defense against viral pathogens. $CD169^+$ macrophages are shown to activate innate and adaptive immunity via "enforced virus replication" a controlled amplification of virus particles. However, factors regulating the $CD169^+$ macrophages remain to be studied. In this paper, we show that after Vesicular stomatitis virus infection, phagocytes produce tumor necrosis factor (TNF) which signals via TNFR1 and promote "enforced virus replication" in

59 CD169$^{+}$ macrophages. Consequently, lack of TNF or TNFR1 resulted in defective immune
60 activation and VSV clearance.





Journal of Virology JVI Journal of Virology

## Introduction

Innate immune activation is crucial for inducing antiviral immunity through cytokine production and adaptive immune priming (1). Splenic marginal zone macrophages and metallophilic marginal zone macrophages play an important role in eliminating blood borne bacterial, parasites and viral pathogens (2, 3). Metallophilic macrophages were originally described when rat splenic marginal zone macrophages were stained with iron and silver impregnation (4). These metallophilic macrophages express the lectin like hemagglutinin CD169, which was identified using a monoclonal antibody: MOMA-1 (5-7). $CD169^+$ macrophages are increasingly recognized to play a pivotal role in host defense (8). $CD169^+$ macrophages (referred to as $CD169^+$ cells), specifically allow early viral replication to promote innate immune recognition and antigen presentation (9). The absence of $CD169^+$ cells results in reduced type I interferon (IFN-I) production, reduced B-cell activation, and severe disease development during viral infection (10, 11). B cell–derived lymphotoxin alpha (Lt$\alpha$) and lymphotoxin beta (LT$\beta$) drive the maintenance of $CD169^+$ cells in spleen and lymph node tissue (10, 12, 13). Consequently, B cell–deficient mice exhibit fewer $CD169^+$ cells and limited immune activation, including the production of IFN-I (13, 14). However, factors promoting survival and the presence of $CD169^+$ cells after viral infection have not yet been sufficiently studied.

IFN-I triggers strong inhibitory effects on viral replication and is crucial for preventing severe infections with the vesicular stomatitis virus (VSV) model system (1, 15). This system can be used as a laboratory system for immune recognition during viral infection, as a vaccine vector system, as a tool for viral transduction, and as an oncolytic virus (16, 17). Clearance of VSV depends heavily on IFN-I and the presence of neutralizing

antibodies (15, 18). VSV has been used as a murine model of viral infections to study the innate immune response, virus replication in secondary lymphoid organs and the central nervous system (CNS) (19-21). Pathology during VSV infection is seen particularly during infection of the central nervous system (CNS); this pathology includes paralysis and death after infection with VSV (22). Accordingly, mice deficient in IFN-α/β receptor (IFNAR) signaling exhibit paralysis and the presence of VSV in the CNS (15). Consistently, IFN-I can inhibit VSV replication in neurons, and defects in IFN-stimulated genes in the CNS tissue trigger pathology during VSV infection (23, 24). During infection with low doses of VSV, replication of VSV in $CD169^{+}$ cells in the spleen and lymph node tissue is important for inducing protective immunity and preventing CNS infection (9, 10). The VSV backbone is also used during vaccination to induce protective immunity against viruses such as the Ebola virus (25).

The role of tumor necrosis factor (TNF) in marginal zone development and marginal zone function is controversial. Although reports show that marginal zone development is impaired and fewer marginal zone macrophages are present in TNF-deficient and p55-TNFR (tumor necrosis factor receptor 1 [TNFR1])-deficient mice (26), other reports suggest that TNF triggers marginal zone macrophage depletion after infection (27, 28). It has also been shown that TNFR1 deficient mice are less susceptible to West Nile virus infection as a result of uncompromised blood brain barrier (29). However, these findings are contradicting other studies utilizing Herpes simplex virus-1 as infection model where it is shown that TNFR1 deficient mice are more susceptible to virus infection (30, 31). It is clear that TNF-deficient mice exhibit $CD169^{+}$ cells in the spleen, whereas this cell population is absent in $Lt\alpha^{-/-}$ mice (26, 27). Furthermore, the production of neutralizing antibodies and the proliferation of

107 antiviral T cells can be induced in TNF-deficient animals (28, 32). These findings suggest
108 that TNF, which is crucial for overcoming bacterial infections (33-36) plays a minor role in
109 antiviral immunity.

110 In this study, we found that absence of TNF reduced the number of $CD169^{+}$ cells,
111 inhibited IFN-I production, and consequently led to a severe disease outcome during
112 infection with VSV. These effects were mainly transmitted by TNFR1 and were dependent
113 on canonical nuclear factor (NF)-κB.

## Results

### TNF production by CD11b$^+$Ly6C$^+$Ly6G$^+$ cells following VSV infection.

TNF can be detected during an infection with VSV (32, 37). Consistently, we found that TNF expression levels were higher in the spleen after infection with VSV when compared to uninfected controls (Fig. 1A). Backgating of intracellular TNF producing cells showed that TNF-producing cells are a heterogeneous CD11b$^+$ CD19$^-$ population (Fig. 1B+C). Therefore, we hypothesized that TNF was likely not expressed by B or T cells during infection. Accordingly, we observed TNF mRNA expression levels in *Cd8*$^{-/-}$, B cell–deficient *Jh*$^{-/-}$, and *Rag1*$^{-/-}$ mice comparable to WT mice (Fig. 1D). TNF producing cells could be predominantly characterized as CD11b$^+$CD11c$^-$Ly6C$^+$Ly6G$^+$MHCII$^-$ (Fig. 1E). Consistent with reports that neutrophils (38, 39) and CD11b$^+$Ly6C$^+$Ly6G$^+$ cells (40) are important during early defense against bacterial and viral infections via production of proinflammatory cytokines such as IL1b, IL6, TNF and IFN-I, we found a significant increase of TNF$^+$CD11b$^+$Ly6C$^+$Ly6G$^+$ cells (Fig. 1F). Treatment with clodronate liposomes can deplete phagocytic cells in mice (Fig. 1G)(41, 42). Accordingly, clodronate depletion reduced TNF expression after VSV infection suggesting a role of these phagocytic cells in the production of TNF (Fig. 1H). However, when we employed diphtheria toxin- receptor (DTR) induced specific cell depletion of CD169$^+$ cells and CD11c$^+$ cells; we did not observe reduction in TNF production (Fig.1H). Taken together, these findings indicate that TNF production following intravenous VSV infection is triggered by CD11b$^+$CD11c$^-$Ly6C$^+$Ly6G$^+$ phagocytes.

**TNF triggers the maintenance of CD169$^+$ cells during viral infection to protect animals against the development of severe disease**

To determine whether TNF affects the outcome after VSV infection, we infected wild-type (WT) and TNF-deficient mice. TNF-deficient mice developed severe VSV infection in comparison to WT mice (Fig. 2A). Neutralizing antibody titer was achieved later in TNF-deficient mice than in WT mice after infection with low doses of VSV (Fig. 2B). Since IFN-I is critical to overcome an infection with VSV (15), we measured IFN alpha and IFN beta in the serum of infected animals. IFN alpha production was impaired in TNF-deficient mice when compared to control animals (Fig. 2C). However, IFN beta was undetectable in the serum of infected animals when infected with $10^5$ PFU VSV (Fig. 2C). Previous findings show that CD169$^+$ cells contribute to innate immune activation not only by allowing viral replication but also by producing IFN-I in mice (10, 43). When we depleted CD169$^+$ cells expressing diphtheria toxin receptor (CD169-DTR) by administering diphtheria toxin (DT) (44), we observed reduced IFN-I concentrations in the serum of infected animals (Fig. 2D). To exclude the possibility of defective innate Toll-like receptor (TLR) activation, we administered the TLR3 agonist poly I:C. We found that the IFN-I production was intact in both WT and TNF-deficient mice (Fig. 2E). Hence, we speculated that TNF promoted the function of CD169$^+$ cells and thus contributed to IFN-I production following VSV infection. Shortly after infection with VSV, the number of CD169$^+$ cells in spleen tissue decreased in TNF-deficient mice when compared to spleen tissue harvested from WT animals (Fig. 2F-H). To understand the reduced production of IFN-I in absence of TNF, we monitored the virus replication in spleen tissue of WT and *Tnfa*$^{-/-}$ mice. The expression of VSV glycoprotein (VSV-G) was detected in lower quantities in spleen tissue harvested from TNF-deficient

159 animals compared to WT mice after VSV infection (Fig. 2I+J). Consistently, early VSV titers
160 after infection were lower in *Tnfa*$^{-/-}$ mice than in control mice, a condition that negatively
161 affects antiviral immune activation (Fig. 2K). Injection of ultraviolet light (UV)-inactivated
162 virus could increase TNF mRNA expression in WT mice (Fig. 2L). However, decrease of
163 CD169$^{+}$ cells was dependent on live virus, because UV-inactivated virus did not affect
164 CD169$^{+}$ cells in spleen tissue of *Tnfa*$^{-/-}$ mice (Fig. 2M). These findings indicate that TNF is
165 necessary to sustain virus replication in early hours of infection but is dispensable for sterile
166 innate immune activation. Notably, *CD169*$^{-/-}$ mice exhibited VSV-G expression in spleen
167 tissue, a finding indicating that downregulation of the protein CD169 would not cause
168 absence of virus replication (Fig. 2N). Taken together, these findings indicate that the
169 absence of TNF results in defective antiviral innate immune activation after infection with
170 VSV.

171

172 **CD169$^{+}$ cell maintenance via TNFR1 results in productive VSV replication and**
173 **immune activation**

174 To further characterize the role of TNF during viral infection, we infected TNFR1-
175 and TNFR2-deficient mice with VSV. In line with findings from TNF-deficient animals, the
176 absence of TNFR1 but not that of TNFR2 resulted in a decrease in the number of CD169$^{+}$
177 cells in spleen tissue (Fig. 3A + B). Furthermore, VSV-G production was lower in *Tnfrsf1a*$^{-/-}$
178 animals than in WT or *Tnfrsf1b*$^{-/-}$ mice (Fig. 3A). Consistently, VSV titers were reduced in
179 spleen tissue shortly after infection in *Tnfrsf1a*$^{-/-}$ animals, in sharp contrast to the findings in
180 WT and *Tnfrsf1b*$^{-/-}$ mice (Fig. 3C). Interestingly, IFN-I production was defective in *Tnfrsf1a*$^{-}$

181 $^{-/-}$ mice but was also lower in *Tnfrsf1b*$^{-/-}$ animals than in WT control mice (Fig. 3D). IFN-I is
182 necessary for the expression of anti-virally active IFN-stimulated genes (ISGs) (1).
183 Consistently, we found reduced expression of ISGs in the CNS of *Tnfrsf1a*$^{-/-}$ mice after
184 infection with VSV (Fig. 3E). Defective ISG expression was not found to the same extent in
185 *Tnfrsf1b*$^{-/-}$ CNS tissue (Fig. 3F). VSV can drive neuropathological symptoms by infecting
186 the CNS (22). When we measured viral titers in the spinal cord and brain tissue of mice
187 exhibiting hind leg paralysis, we found infectious VSV in tissue from TNFR1-deficient mice
188 (Figure 3G). Consequently, *Tnfrsf1a*$^{-/-}$ mice developed clinical signs of CNS infection,
189 unlike WT and *Tnfrsf1b*$^{-/-}$ mice (Fig. 3H). Taken together, these findings suggest that TNFR1
190 drives antiviral defense by promoting CD169$^{+}$ cell survival.

191

192 **TNFR1 triggers the survival of CD169$^{+}$ cells**

193 Next, we opted to determine which factors drive the maintenance of CD169$^{+}$ cells and
194 enforced viral replication after viral infection. B cell–mediated Ltβ production is important
195 for splenic CD169$^{+}$ cells. Hence, we wondered whether the defects in absence of TNF were
196 triggered by B cells. Notably, we did not observe any major changes of B-cell subsets in
197 TNF, TNFR1 or TNFR2-deficient mice (Fig. 4A). Consistently, we did not see differential
198 expression of *Lt*α, *Lt*β, or Ltβ receptor (*LtbR*) in TNFR1-deficient mice (Fig. 4B).
199 Additionally, we found no major differences in B-cell subsets between WT and *Tnfrsf1a*$^{-/-}$
200 mice after infection (Fig. 4C). Furthermore, we reconstituted lethally irradiated C57BL/6
201 mice with mixed bone marrow from *Rag1*$^{-/-}$ and *Tnfrsf1a*$^{-/-}$ and *Rag1*$^{-/-}$ and WT donors at a
202 ratio of 1:1. Mice reconstituted with *Rag1*$^{-/-}$: *Tnfrsf1a*$^{-/-}$ bone marrow exhibited no

significant reduction in IFN-α in the serum when compared to mice reconstituted with *Rag1*$^{-/-}$: WT bone marrow (Fig. 4D). Furthermore, there was no difference between these mice in neutralizing antibody production (Fig. 4E). To elucidate if TNFR1 deficiency specifically on CD169$^{+}$ cells have a role in virus replication, we reconstituted lethally irradiated C57BL/6 mice with mixed bone marrow from CD169-DTR$^{+}$ and *Tnfrsf1a*$^{-/-}$ donors as well as CD169-DTR$^{+}$ and WT donors at a ratio of 1:1. We observed that the production of IFN-α was lower in the mice reconstituted with CD169-DTR$^{+}$ + *Tnfrsf1a*$^{-/-}$ bone marrow compared to control mice reconstituted with CD169-DTR$^{+}$ + WT after infection with VSV and DT treatment (Fig. 4F). Furthermore, we found slightly delayed presence of VSV neutralizing antibody titers in CD169-DTR$^{+}$:*Tnfrsf1a*$^{-/-}$ recipients when compared to corresponding CD169-DTR$^{+}$:WT recipients (Fig. 4G). CD169$^{+}$ cells can be depleted in CD11c-DTR mice, because CD169$^{+}$ cells exhibit intermediate expression of CD11c (10, 45). Consistently, lethally irradiated mice reconstituted with mixed bone marrow from CD11c-DTR$^{+}$ and *Tnfrsf1a*$^{-/-}$ mice exhibited reduced concentrations of IFN-α after VSV infection when compared to CD11c-DTR$^{+}$ :WT recipients (Fig. 4H). These findings suggest that TNFR1 triggers cell-intrinsic effects on CD169$^{+}$ cells.

We speculated that TNF delivers an important survival signal for CD169$^{+}$ cells. To determine if TNF is involved in protection against VSV induced apoptosis, we measured caspase 3 activity on whole spleen tissue lysates. After VSV infection caspase 3 activity was significantly higher in *Tnfa*$^{-/-}$ mice compared to control animals (Fig. 5A). VSV is known to induce apoptosis and inactivates Mcl-1 and Bcl-Xl (46). To elucidate if TNF plays a role in promoting expression of anti-apoptotic genes, we measured mRNA expression of *Bcl2*, *Bcl-Xl* and *xIAP* in spleen tissue of mice after VSV infection (Fig. 5B). After VSV infection,

226 *Bcl2* and *Bcl-Xl* expression was significantly reduced in *Tnfa*$^{-/-}$ mice compared to WT mice
227 (Fig. 5B). To enumerate the mechanism which reduces CD169$^{+}$ cells in TNF deficient mice
228 after infection we made use of terminal deoxynucleotidyl transferase dUTP nick end
229 labelling (TUNEL) assay. The number as well as the mean fluorescence intensity of TUNEL-
230 positive CD169$^{+}$ cells was higher in spleen tissue from TNF deficient mice than in tissue
231 from corresponding WT control mice (Fig. 5C+D). The proportion of CD169$^{+}$ cells that
232 stained positive for *7*-aminoactinomycin D (7-AAD) was higher in TNFR1-deficient mice
233 than in WT control mice 8h after infection (Fig. 5E). Next, we wondered if we can rescue the
234 CD169$^{+}$ cells by injecting the pan-caspase inhibitor Z-Val-Ala-Asp-fluoromethylketone
235 (zVAD-FMK). Z-VAD treatment restored the presence of CD169$^{+}$ cells in TNF-deficient
236 animals, a finding indicating that CD169$^{+}$ cells depend on TNF-mediated survival (Fig.
237 5F+G). Although treatment of TNF-deficient mice with Z-VAD rescued CD169$^{+}$ cells, it
238 failed to rescue the IFN-I response suggesting the role of TNF signaling is not only essential
239 to prevent apoptosis, but also for IFN-I production (Fig. 5H). In summary, these findings
240 indicate that TNF delivers a survival signal that is important for the maintenance of CD169$^{+}$
241 cells in the spleen after viral infection and IFN-I production.

242

243 **The NF-κB regulator MALT1 promotes canonical NF-κB expression, VSV replication**
244 **in CD169$^{+}$ cells, and immune activation during viral infection**

245 TNF can induce NF-κB activation via TNFR1 and can promote the expression of
246 genes driving survival and of proinflammatory cytokines (47). Furthermore, TNF is known to
247 promote IFN-I production (48). Consistently, RelA expression was increased in the marginal

248 zone of spleen tissue after VSV infection (Fig. 6A). We quantified cytoplasmic and nuclear
249 expression of RelA in CD169$^{+}$ cells. Nuclear presence of RelA in CD169$^{+}$ cells was higher in
250 VSV-infected mice than in naïve controls (Fig. 6B). We wondered whether nuclear *RelA*
251 expression was dependent on TNF. As expected, compared with WT control mice, VSV-
252 infected mice exhibited reduced expression of RelA in the nuclear compartment of CD169$^{+}$
253 cells in absence of TNF (Fig. 6C). Notably, the presence of RelA was reduced in TNFR1
254 deficient mice, but we observed no difference in RelA expression between TNFR2-deficient
255 mice and corresponding control mice (Fig. 6D+E). It has been reported that one of the major
256 regulator of RelA signaling is RelB which acts through sequestration of RelA in the
257 cytoplasm and competitive binding of DNA (49). It is also reported that the paracaspase
258 MALT1 can promote canonical NF-κB signaling by cleaving RelB (50, 51). Hence, we
259 stained spleen sections of *Malt1*$^{+/-}$ and *Malt1*$^{-/-}$ mice for RelB. Ablation of MALT1 resulted
260 in increased levels of RelB in CD169$^{+}$ cells in the marginal zone of the spleen (Fig. 7A+B).
261 In turn, nuclear RelA levels were lower in CD169$^{+}$ cells in *Malt1*$^{-/-}$ spleen tissue than in
262 control tissue (Fig. 7C). Consistently, mouse embryonic fibroblasts (MEFs) derived from
263 *Malt1*$^{-/-}$ mice showed reduced translocation of p65 into the nucleus after stimulation with
264 TNF but higher expression of RelB in the nucleus (Fig. 7D+E). These findings indicate that
265 MALT1 destabilizes RelB in marginal zone macrophages to promote canonical NF-κB
266 signaling. The presence of CD169$^{+}$ cells in spleen tissue was not affected by *Malt1* before or
267 after infection with VSV (Fig. 8A). However, the expression of VSV-G was lower in *Malt1*$^{-/-}$
268 mice than in control mice (Fig. 8B+C). Consistently, the number of infectious VSV particles
269 were lower in spleen tissue harvested from *Malt1*$^{-/-}$ mice than in spleen tissue from control
270 mice (Fig. 8D). Hence, IFN-I serum concentrations after VSV infection were lower in

MALT1 deficient mice than in control mice (Fig. 8E). A previous report suggests that MALT1 is not required for RIG-I activation (52). Consistently, when we injected polyI:C into *Malt1*$^{+/-}$ and *Malt1*$^{-/-}$ mice, we found similar serum IFN-I levels in both groups (Fig. 8F). Hence we concluded that defective IFN-I production during VSV infection was caused by reduced VSV replication early during infection. Consequently, MALT1 deficient mice succumbed to the infection in sharp contrast to control animals (Fig. 8G).

Taken together, these findings indicate that absence of MALT1 results in reduced canonical NF-κB signaling in response to VSV infection. *Malt1*-deficient mice exhibit reduced VSV replication and immune activation.

**Discussion**

In this study, we found that TNF plays a crucial role in the maintenance of $CD169^+$ cells early after infection with VSV. Consequently, TNF, TNFR1, and MALT1 deficient animals exhibited reduced immune activation, limited IFN-I production, which consequently led to a sever VSV infection.

The role of TNF during viral infection is controversial and not sufficiently understood. Although reports describe activating polymorphisms in TNF, which are associated with the establishment of a chronic viral infection (53), other reports state that the same mutations are protective against chronic hepatitis B virus infection (HBV) (54). *In vitro*, TNF can propagate the viral replication of HCV (55) although HCV increases the incidence of TNF-induced apoptosis (56). On the other hand, TNF strongly inhibits influenza virus replication in porcine lung epithelial cells (57). Consistently, the attenuation of TNF signaling in a murine T cell–independent model of HBV infection results in viral persistence (58). In turn, the application of Smac mimetics enhances TNF signaling and is associated with increased clearance of HBV in this model system (59). During infection with VSV, the production of neutralizing antibodies is not defective in the absence of TNFR1 (32). Moreover, TNF can induce T-cell dysfunction and, therefore, promote chronic viral infection (60). Our findings that TNF is crucial for the maintenance of $CD169^+$ cells in spleen tissue may be important for infections with lower doses of virus, because allowing viral replication in $CD169^+$ cells is particularly important for protective adaptive immunity (9, 13). This may be crucial for the maintenance of $CD169^+$ cells in spleen tissue during vaccination with attenuated virus strains or VSV vector–based vaccines (25). These findings may not only be

specific for splenic CD169$^+$ cells, since intranasal infection with recombinant TNF overexpressing Rabies virus (RV), reduced RV load and mortality (61).

Viral replication in CD169$^+$ cells, which is promoted by TNF, contributes to improved antigen presentation. CD169$^+$ cells in the marginal zone are in close contact with pathogens and are ideally situated to induce an immune response (62). Furthermore, CD169$^+$ cells have been shown not only to present antigens to B cells in the lymph nodes but also to prime T cells (11, 63). Moreover, CD169$^+$ cells are important for virus-mediated IFN-I production which prevents severe CNS infection in mice (64). Our findings show that TNF promotes maintenance of CD169$^+$ cells and IFN-I production following VSV infection. Furthermore, our findings show that the translocation of RelA to the nuclei of CD169$^+$ cells after VSV infection is dependent on TNF. It has been postulated that canonical NF-κB can contribute to the production of IFN-α (65, 66). However, RelA-deficient and p50-deficient MEFs can produce IFN-α after viral infection, whereas only early IFN-I transcription is reduced (67, 68). Furthermore, RelA-deficient plasmacytoid dendritic cells (pDCs) exhibited reduced IFN production after exposure to Sendai virus (69). Our findings indicate that canonical NF-κB activation can also promote early viral replication and consequently contribute to the production of IFN-I. Consistently, non-canonical NF-κB, which can inhibit canonical NF-κB signaling, is a potent inhibitor of IFN-I production (70). Hence, the paracaspase MALT1, which can cleave RelB and consequently promote canonical NF-κB signaling (50, 51) is necessary for the sufficient propagation of VSV replication and IFN-I production.

Taken together, we have found that TNF-TNFR1 signaling is crucial for protecting CD169$^+$ cells and their function in innate immune activation during VSV infection.

**Materials and Methods:**

**Mice, viruses, virus titration:** *Tnfa*$^{-/-}$, *Tnfrsf1b*$^{-/-}$, *Cd8*$^{-/-}$ and *Rag1*$^{-/-}$ mice were purchased from Jackson Laboratories (United States). *Tnfrsf1a*$^{-/-}$ mice have been previously described (34). *Malt1*$^{-/-}$, *CD169*$^{-/-}$, CD169-DTR, and CD11c-DTR mice have also been previously described (71-74). All mice were maintained on a C57BL/6 genetic background. VSV Indiana strain (VSV-IND, strain Mudd-Summers) was originally obtained from Prof. D. Kolakofsky (University of Geneva, Switzerland). VSV was propagated and titrated as previously described (13). Mice were infected with VSV via tail vein injection. In survival experiments, mice exhibiting symptoms of hind leg paralysis were considered severe, taken out of the experiment, and counted as dead. Blood was collected at the indicated time points after infection. VSV neutralizing antibody titers were measured by plaque reduction neutralization test (PRNT) as previously described (9, 13). Briefly, serum samples were diluted 1:40 and incubated at 56ºC for 30 min. To evaluate IgG, serum was pretreated with 0.1M β-mercaptoethanol. Serial 2 fold dilutions were performed for 12 steps and incubated with 5000 PFU of VSV. Virus and serum mixture was incubated on a Vero cell monolayer. Plates were stained with crystal violet after 24h. To inhibit caspase activity *in vivo*, we administered three doses (2 µg/g each) of zVAD-FMK (Abcam, Cambridge, UK) (75, 76). For chimera experiments, mice were lethally irradiated with 10.2 Gy. After 24 h, mixed bone marrow from WT or *Tnfrsf1a*$^{-/-}$ and CD169-DTR, CD11c-DTR, and *Rag1*$^{-/-}$ mice was transplanted into the irradiated mice as indicated. All mice were maintained under specific pathogen–free conditions at the authorization of the Landesamt für Natur, Umwelt und Verbraucherschutz of North Rhine-Westphalia (LANUV NRW) in accordance with the German laws for animal protection.

348 **Depletion of cells:** To deplete macrophages, 200ul clodronate liposomes was injected
349 intravenously, 24h later mice were infected with VSV. Clodronate was provided by Nico van
350 Rooijen and used as previously described (41, 42)(Vrije University Medical Center,
351 Netherlands). $CD169^+$ and $CD11c^+$ expressing cells in CD169-DTR and CD11c-DTR mice
352 were depleted by injecting 2 doses of 100ng diphtheria toxin (DT) (Sigma) 1 day before and
353 at the day of infection.

354

355 **Histology and ELISA:** Histological analysis of snap-frozen tissue was performed as
356 previously described (9). Briefly, Snap-frozen tissue sections were cut in 7µm thickness, air
357 dried and fixed with acetone for 10min. Sections were blocked with 2% fetal calf serum in
358 PBS for 1h. Sections were stained with anti-CD169 (final conc. 4 µg/ml) (Acris, Germany;
359 clone: MOMA-1), anti-VSV-G (final conc. 1 µg/ml) (produced in-house, clone: Vi10), anti-
360 RelA (final conc. 1µg/ml) (Santa Cruz Biotechnology, USA), anti-F4/80 (final conc. 2µg/ml)
361 (eBioscience, clone BM8) and anti-RelB (final conc. 1µg/ml) (Cell Signaling, USA;
362 polyclonal) for 1h. Then Sections were washed with PBS containing 0.05% Tween 20
363 (Sigma). Secondary antibodies, PE streptavidin (final conc. 1µg/ml) (eBioscience), anti-
364 Rabbit FITC (final conc. 1µg/ml) (Thermofisher), anti-Goat FITC (final conc. 1µg/ml) (Santa
365 Cruz Biotechnology, USA) were incubated for 1h. Then sections were washed with PBS
366 containing 0.05% Tween 20 (Sigma) and mounted using fluorescence mounting medium
367 (Dako). Caspase 3 activity assay was performed with a fluorescence assay according to the
368 manufacturer's instructions (Cell Signaling). TUNEL staining was performed on formalin-
369 fixed spleen sections according to the manufacturer's instructions (Thermo scientific, USA).
370 Images were obtained with a LSM510 confocal microscope and Axio Observer Z1

371 fluorescence microscope (Zeiss, Germany). Analysis of the fluorescence images was
372 performed with ImageJ software. IFN-α and IFN-β (PBL Biosciences, New Jersey, USA)
373 concentrations were determined using enzyme-linked immunosorbent assay (ELISA)
374 according to the manufacturers' instructions.

375 **RT-PCR analyses:** RNA purification was performed according to manufacturer's
376 instructions (Qiagen RNeasy Kit or Trizol). Gene expression of *Bcl2, Bcl-xl, Xiap, Lta, Ltb,*
377 *Ifit1, Ifit2, Ifit3, Irf7, Isg15, Oasl1 and Tnfa,* was performed using FAM/VIC probes (Applied
378 Biosystems) and iTAQ™ One step PCR kit (Bio rad). For analysis, the expression levels of
379 all target genes were normalized to β-actin/GAPDH expression (ΔCt). Gene expression
380 values were then calculated based on the ΔΔCt method, using naive WT mice as a control to
381 which all other samples were compared. Relative quantities (RQ) were determined using the
382 equation: RQ=2^-ΔΔCt.

383 **Immunoblotting:** *Malt1*$^{+/-}$ and *Malt1*$^{-/-}$ mouse embryonic fibroblasts (MEFs) were obtained
384 from Jürgen Ruland (Technische Universität München, Germany). *Malt1*$^{+/-}$ and *Malt1*$^{-/-}$
385 MEFs were stimulated with 100 ng/ml murine-soluble TNF (mTNF; R&D Systems).
386 Cytoplasmic and nuclear extracts were prepared according to manufacturer's instructions
387 (Active Motif, Belgium). Immunoblots were probed with primary anti-p65 (Santa Cruz
388 Biotechnology), anti-RelB (Cell Signaling), and anti-p100/p52 (Cell Signaling).

389 **Flow cytometry:** For intracellular cytokine staining, single-cell suspended splenocytes were
390 incubated with Brefeldin A (eBioscience), followed by an additional 5 h of incubation at
391 37°C. After surface staining with anti-CD3, anti-CD8, anti-CD11b, anti-CD11c, anti-CD19,

anti-CD115, anti-F4/80, anti-Ly6C, anti-Ly6G anti-MHC-II, and anti-NK1.1 antibodies (all from eBioscience), cells were fixed with 2% formalin, permeabilized with 0.1% saponin, and stained with anti-TNF antibodies (eBioscience) for 30 min at 4°C. B-cell subsets were detected in single-cell suspensions of splenocytes with anti-CD5, anti-CD19, anti-CD21, anti-CD23, and anti–immunoglobulin M (IgM) antibodies (all from eBioscience). BD Calibrite™ (BD Biosciences, USA) beads were added to the samples before acquisition by BD LSRFortessa™.

**Statistical analyses:** Data are represented as +SEM or ±SEM. Statistically significant differences between two groups were determined with Student's *t*-test. Statistically significant differences between several groups were determined by one-way analysis of variance (ANOVA) with additional Bonferroni or Dunnett post hoc test. Statistically significant differences between groups in experiments involving more than one time-point were determined with two-way ANOVA (repeated measurements).

**Acknowledgements:**

We thank Flo Witte for valuable comments on the manuscript. This study was supported by the Alexander von Humboldt Foundation (SKA2010), the German Research Council (SFB974, LA2558/3-1, LA2558/5-1, GRK1949 & TRR60), the Jürgen Manchot Graduate School MOI II, and the NIH tetramer facility. D.B.is funded by the ATTRACT Programme (A14/BM/7632103/DBRRIL) and a CORE grant (C15/BM/10355103) of the National Research Fund Luxembourg (FNR).

**References:**


1. McNab F, Mayer-Barber K, Sher A, Wack A, O'Garra A. 2015. Type I interferons in infectious disease. Nat Rev Immunol 15:87-103.
2. Chavez-Galan L, Olleros ML, Vesin D, Garcia I. 2015. Much More than M1 and M2 Macrophages, There are also CD169(+) and TCR(+) Macrophages. Front Immunol 6:263.
3. Mebius RE, Kraal G. 2005. Structure and function of the spleen. Nat Rev Immunol 5:606-16.
4. Snook T. 1964. Studies on the Perifollicular Region of the Rat's Spleen. Anat Rec 148:149-59.
5. Crocker PR, Gordon S. 1986. Properties and distribution of a lectin-like hemagglutinin differentially expressed by murine stromal tissue macrophages. J Exp Med 164:1862-75.
6. Kraal G, Janse M. 1986. Marginal metallophilic cells of the mouse spleen identified by a monoclonal antibody. Immunology 58:665-9.
7. Oetke C, Kraal G, Crocker PR. 2006. The antigen recognized by MOMA-I is sialoadhesin. Immunol Lett 106:96-8.
8. Gupta P, Lai SM, Sheng J, Tetlak P, Balachander A, Claser C, Renia L, Karjalainen K, Ruedl C. 2016. Tissue-Resident CD169(+) Macrophages Form a Crucial Front Line against Plasmodium Infection. Cell Rep 16:1749-61.
9. Honke N, Shaabani N, Cadeddu G, Sorg UR, Zhang DE, Trilling M, Klingel K, Sauter M, Kandolf R, Gailus N, van Rooijen N, Burkart C, Baldus SE, Grusdat M, Lohning M, Hengel H, Pfeffer K, Tanaka M, Haussinger D, Recher M, Lang PA, Lang KS. 2012. Enforced viral replication activates adaptive immunity and is essential for the control of a cytopathic virus. Nature Immunology 13:51-7.
10. Iannacone M, Moseman EA, Tonti E, Bosurgi L, Junt T, Henrickson SE, Whelan SP, Guidotti LG, von Andrian UH. 2010. Subcapsular sinus macrophages prevent CNS invasion on peripheral infection with a neurotropic virus. Nature 465:1079-83.
11. Junt T, Moseman EA, Iannacone M, Massberg S, Lang PA, Boes M, Fink K, Henrickson SE, Shayakhmetov DM, Di Paolo NC, van Rooijen N, Mempel TR, Whelan SP, von Andrian UH. 2007. Subcapsular sinus macrophages in lymph nodes clear lymph-borne viruses and present them to antiviral B cells. Nature 450:110-4.
12. Tumanov A, Kuprash D, Lagarkova M, Grivennikov S, Abe K, Shakhov A, Drutskaya L, Stewart C, Chervonsky A, Nedospasov S. 2002. Distinct role of surface lymphotoxin expressed by B cells in the organization of secondary lymphoid tissues. Immunity 17:239-50.
13. Xu HC, Huang J, Khairnar V, Duhan V, Pandyra AA, Grusdat M, Shinde P, McIlwain DR, Maney SK, Gommerman J, Lohning M, Ohashi PS, Mak TW, Pieper K, Sic H, Speletas M, Eibel H, Ware CF, Tumanov AV, Kruglov AA, Nedospasov

SA, Haussinger D, Recher M, Lang KS, Lang PA. 2015. Deficiency of the B cell-activating factor receptor results in limited CD169+ macrophage function during viral infection. J Virol 89:4748-59.

14. Khairnar V, Duhan V, Maney SK, Honke N, Shaabani N, Pandyra AA, Seifert M, Pozdeev V, Xu HC, Sharma P, Baldin F, Marquardsen F, Merches K, Lang E, Kirschning C, Westendorf AM, Haussinger D, Lang F, Dittmer U, Kuppers R, Recher M, Hardt C, Scheffrahn I, Beauchemin N, Gothert JR, Singer BB, Lang PA, Lang KS. 2015. CEACAM1 induces B-cell survival and is essential for protective antiviral antibody production. Nat Commun 6:6217.
15. Muller U, Steinhoff U, Reis LF, Hemmi S, Pavlovic J, Zinkernagel RM, Aguet M. 1994. Functional role of type I and type II interferons in antiviral defense. Science 264:1918-21.
16. Kawai T, Akira S. 2009. The roles of TLRs, RLRs and NLRs in pathogen recognition. Int Immunol 21:317-37.
17. Lichty BD, Power AT, Stojdl DF, Bell JC. 2004. Vesicular stomatitis virus: re-inventing the bullet. Trends Mol Med 10:210-6.
18. Hangartner L, Zinkernagel RM, Hengartner H. 2006. Antiviral antibody responses: the two extremes of a wide spectrum. Nat Rev Immunol 6:231-43.
19. Bi Z, Barna M, Komatsu T, Reiss CS. 1995. Vesicular stomatitis virus infection of the central nervous system activates both innate and acquired immunity. J Virol 69:6466-72.
20. Chauhan VS, Furr SR, Sterka DG, Jr., Nelson DA, Moerdyk-Schauwecker M, Marriott I, Grdzelishvili VZ. 2010. Vesicular stomatitis virus infects resident cells of the central nervous system and induces replication-dependent inflammatory responses. Virology 400:187-96.
21. Christian AY, Barna M, Bi Z, Reiss CS. 1996. Host immune response to vesicular stomatitis virus infection of the central nervous system in C57BL/6 mice. Viral Immunol 9:195-205.
22. Huneycutt BS, Bi Z, Aoki CJ, Reiss CS. 1993. Central neuropathogenesis of vesicular stomatitis virus infection of immunodeficient mice. J Virol 67:6698-706.
23. Fensterl V, Wetzel JL, Ramachandran S, Ogino T, Stohlman SA, Bergmann CC, Diamond MS, Virgin HW, Sen GC. 2012. Interferon-induced Ifit2/ISG54 protects mice from lethal VSV neuropathogenesis. PLoS Pathog 8:e1002712.
24. Trottier MD, Jr., Palian BM, Reiss CS. 2005. VSV replication in neurons is inhibited by type I IFN at multiple stages of infection. Virology 333:215-25.
25. Jones SM, Feldmann H, Stroher U, Geisbert JB, Fernando L, Grolla A, Klenk HD, Sullivan NJ, Volchkov VE, Fritz EA, Daddario KM, Hensley LE, Jahrling PB, Geisbert TW. 2005. Live attenuated recombinant vaccine protects nonhuman primates against Ebola and Marburg viruses. Nat Med 11:786-90.
26. Pasparakis M, Kousteni S, Peschon J, Kollias G. 2000. Tumor necrosis factor and the p55TNF receptor are required for optimal development of the marginal sinus and for migration of follicular dendritic cell precursors into splenic follicles. Cell Immunol 201:33-41.
27. Engwerda CR, Ato M, Cotterell SE, Mynott TL, Tschannerl A, Gorak-Stolinska PM, Kaye PM. 2002. A role for tumor necrosis factor-alpha in remodeling the splenic marginal zone during Leishmania donovani infection. Am J Pathol 161:429-37.

28. Calzascia T, Pellegrini M, Hall H, Sabbagh L, Ono N, Elford AR, Mak TW, Ohashi PS. 2007. TNF-alpha is critical for antitumor but not antiviral T cell immunity in mice. J Clin Invest 117:3833-45.
29. Wang T, Town T, Alexopoulou L, Anderson JF, Fikrig E, Flavell RA. 2004. Toll-like receptor 3 mediates West Nile virus entry into the brain causing lethal encephalitis. Nat Med 10:1366-73.
30. Lundberg P, Welander PV, Edwards CK, 3rd, van Rooijen N, Cantin E. 2007. Tumor necrosis factor (TNF) protects resistant C57BL/6 mice against herpes simplex virus-induced encephalitis independently of signaling via TNF receptor 1 or 2. J Virol 81:1451-60.
31. Vilela MC, Lima GK, Rodrigues DH, Lacerda-Queiroz N, Mansur DS, de Miranda AS, Rachid MA, Kroon EG, Vieira LQ, Campos MA, Teixeira MM, Teixeira AL. 2010. TNFR1 plays a critical role in the control of severe HSV-1 encephalitis. Neurosci Lett 479:58-62.
32. Fehr T, Bachmann MF, Bluethmann H, Kikutani H, Hengartner H, Zinkernagel RM. 1996. T-independent activation of B cells by vesicular stomatitis virus: no evidence for the need of a second signal. Cell Immunol 168:184-92.
33. Rothe J, Lesslauer W, Lotscher H, Lang Y, Koebel P, Kontgen F, Althage A, Zinkernagel R, Steinmetz M, Bluethmann H. 1993. Mice lacking the tumour necrosis factor receptor 1 are resistant to TNF-mediated toxicity but highly susceptible to infection by Listeria monocytogenes. Nature 364:798-802.
34. Pfeffer K, Matsuyama T, Kundig TM, Wakeham A, Kishihara K, Shahinian A, Wiegmann K, Ohashi PS, Kronke M, Mak TW. 1993. Mice deficient for the 55 kd tumor necrosis factor receptor are resistant to endotoxic shock, yet succumb to L. monocytogenes infection. Cell 73:457-67.
35. Botha T, Ryffel B. 2003. Reactivation of latent tuberculosis infection in TNF-deficient mice. J Immunol 171:3110-8.
36. Wellmer A, Gerber J, Ragheb J, Zysk G, Kunst T, Smirnov A, Bruck W, Nau R. 2001. Effect of deficiency of tumor necrosis factor alpha or both of its receptors on Streptococcus pneumoniae central nervous system infection and peritonitis. Infect Immun 69:6881-6.
37. Bartholdy C, Nansen A, Marker O, Thomsen AR. 1999. Soluble tumour necrosis factor (TNF)-receptor levels in serum as markers of anti-viral host reactivity. Clin Exp Immunol 116:299-306.
38. Brandes M, Klauschen F, Kuchen S, Germain RN. 2013. A systems analysis identifies a feedforward inflammatory circuit leading to lethal influenza infection. Cell 154:197-212.
39. Petrofsky M, Bermudez LE. 1999. Neutrophils from Mycobacterium avium-infected mice produce TNF-alpha, IL-12, and IL-1 beta and have a putative role in early host response. Clin Immunol 91:354-8.
40. Fischer MA, Davies ML, Reider IE, Heipertz EL, Epler MR, Sei JJ, Ingersoll MA, Rooijen NV, Randolph GJ, Norbury CC. 2011. CD11b(+), Ly6G(+) cells produce type I interferon and exhibit tissue protective properties following peripheral virus infection. PLoS Pathog 7:e1002374.
41. Stienstra R, Saudale F, Duval C, Keshtkar S, Groener JE, van Rooijen N, Staels B, Kersten S, Muller M. 2010. Kupffer cells promote hepatic steatosis via interleukin-

1beta-dependent suppression of peroxisome proliferator-activated receptor alpha activity. Hepatology 51:511-22.

42. Van Rooijen N, Sanders A. 1996. Kupffer cell depletion by liposome-delivered drugs: comparative activity of intracellular clodronate, propamidine, and ethylenediaminetetraacetic acid. Hepatology 23:1239-43.

43. Garcia Z, Lemaitre F, van Rooijen N, Albert ML, Levy Y, Schwartz O, Bousso P. 2012. Subcapsular sinus macrophages promote NK cell accumulation and activation in response to lymph-borne viral particles. Blood 120:4744-50.

44. Asano K, Nabeyama A, Miyake Y, Qiu CH, Kurita A, Tomura M, Kanagawa O, Fujii S, Tanaka M. 2011. CD169-positive macrophages dominate antitumor immunity by crosspresenting dead cell-associated antigens. Immunity 34:85-95.

45. Probst HC, Tschannen K, Odermatt B, Schwendener R, Zinkernagel RM, Van Den Broek M. 2005. Histological analysis of CD11c-DTR/GFP mice after in vivo depletion of dendritic cells. Clin Exp Immunol 141:398-404.

46. Pearce AF, Lyles DS. 2009. Vesicular stomatitis virus induces apoptosis primarily through Bak rather than Bax by inactivating Mcl-1 and Bcl-XL. J Virol 83:9102-12.

47. Brenner D, Blaser H, Mak TW. 2015. Regulation of tumour necrosis factor signalling: live or let die. Nat Rev Immunol 15:362-74.

48. Basagoudanavar SH, Thapa RJ, Nogusa S, Wang J, Beg AA, Balachandran S. 2011. Distinct roles for the NF-kappa B RelA subunit during antiviral innate immune responses. J Virol 85:2599-610.

49. Marienfeld R, May MJ, Berberich I, Serfling E, Ghosh S, Neumann M. 2003. RelB forms transcriptionally inactive complexes with RelA/p65. J Biol Chem 278:19852-60.

50. Hailfinger S, Nogai H, Pelzer C, Jaworski M, Cabalzar K, Charton JE, Guzzardi M, Decaillet C, Grau M, Dorken B, Lenz P, Lenz G, Thome M. 2011. Malt1-dependent RelB cleavage promotes canonical NF-kappaB activation in lymphocytes and lymphoma cell lines. Proc Natl Acad Sci U S A 108:14596-601.

51. Brustle A, Brenner D, Knobbe CB, Lang PA, Virtanen C, Hershenfield BM, Reardon C, Lacher SM, Ruland J, Ohashi PS, Mak TW. 2012. The NF-kappaB regulator MALT1 determines the encephalitogenic potential of Th17 cells. J Clin Invest 122:4698-709.

52. Poeck H, Bscheider M, Gross O, Finger K, Roth S, Rebsamen M, Hannesschlager N, Schlee M, Rothenfusser S, Barchet W, Kato H, Akira S, Inoue S, Endres S, Peschel C, Hartmann G, Hornung V, Ruland J. 2010. Recognition of RNA virus by RIG-I results in activation of CARD9 and inflammasome signaling for interleukin 1 beta production. Nature Immunology 11:63-9.

53. Sghaier I, Zidi S, Mouelhi L, Dabbech R, Ghazouani E, Brochot E, Stayoussef M, Yacoubi-Loueslati B. 2015. The relationship between TNF alpha gene polymorphisms (-238/-308), TNF RII VNTR (p75) and outcomes of hepatitis B virus infection in Tunisian population. Gene 568:140-5.

54. Xu J, Zhang S, Zhang Z, Fu L, Zheng Q, Wang J, Lu S, Du J. 2013. TNF-alpha promoter region polymorphisms affect HBV virus clearance in southern Chinese. Clin Chim Acta 425:90-2.

55. Fletcher NF, Sutaria R, Jo J, Barnes A, Blahova M, Meredith LW, Cosset FL, Curbishley SM, Adams DH, Bertoletti A, McKeating JA. 2014. Activated

macrophages promote hepatitis C virus entry in a tumor necrosis factor-dependent manner. Hepatology 59:1320-30.

56. Park J, Kang W, Ryu SW, Kim WI, Chang DY, Lee DH, Park DY, Choi YH, Choi K, Shin EC, Choi C. 2012. Hepatitis C virus infection enhances TNFalpha-induced cell death via suppression of NF-kappaB. Hepatology 56:831-40.

57. Seo SH, Webster RG. 2002. Tumor necrosis factor alpha exerts powerful anti-influenza virus effects in lung epithelial cells. J Virol 76:1071-6.

58. Ebert G, Preston S, Allison C, Cooney J, Toe JG, Stutz MD, Ojaimi S, Scott HW, Baschuk N, Nachbur U, Torresi J, Chin R, Colledge D, Li X, Warner N, Revill P, Bowden S, Silke J, Begley CG, Pellegrini M. 2015. Cellular inhibitor of apoptosis proteins prevent clearance of hepatitis B virus. Proc Natl Acad Sci U S A 112:5797-802.

59. Ebert G, Allison C, Preston S, Cooney J, Toe JG, Stutz MD, Ojaimi S, Baschuk N, Nachbur U, Torresi J, Silke J, Begley CG, Pellegrini M. 2015. Eliminating hepatitis B by antagonizing cellular inhibitors of apoptosis. Proc Natl Acad Sci U S A 112:5803-8.

60. Beyer M, Abdullah Z, Chemnitz JM, Maisel D, Sander J, Lehmann C, Thabet Y, Shinde PV, Schmidleithner L, Kohne M, Trebicka J, Schierwagen R, Hofmann A, Popov A, Lang KS, Oxenius A, Buch T, Kurts C, Heikenwalder M, Fatkenheuer G, Lang PA, Hartmann P, Knolle PA, Schultze JL. 2016. Tumor-necrosis factor impairs CD4(+) T cell-mediated immunological control in chronic viral infection. Nature Immunology 17:593-603.

61. Faber M, Bette M, Preuss MA, Pulmanausahakul R, Rehnelt J, Schnell MJ, Dietzschold B, Weihe E. 2005. Overexpression of tumor necrosis factor alpha by a recombinant rabies virus attenuates replication in neurons and prevents lethal infection in mice. J Virol 79:15405-16.

62. Junt T, Scandella E, Ludewig B. 2008. Form follows function: lymphoid tissue microarchitecture in antimicrobial immune defence. Nat Rev Immunol 8:764-75.

63. Bernhard CA, Ried C, Kochanek S, Brocker T. 2015. CD169+ macrophages are sufficient for priming of CTLs with specificities left out by cross-priming dendritic cells. Proc Natl Acad Sci U S A 112:5461-6.

64. Moseman EA, Iannacone M, Bosurgi L, Tonti E, Chevrier N, Tumanov A, Fu YX, Hacohen N, von Andrian UH. 2012. B cell maintenance of subcapsular sinus macrophages protects against a fatal viral infection independent of adaptive immunity. Immunity 36:415-26.

65. Lenardo MJ, Fan CM, Maniatis T, Baltimore D. 1989. The involvement of NF-kappa B in beta-interferon gene regulation reveals its role as widely inducible mediator of signal transduction. Cell 57:287-94.

66. Hiscott J, Alper D, Cohen L, Leblanc JF, Sportza L, Wong A, Xanthoudakis S. 1989. Induction of human interferon gene expression is associated with a nuclear factor that interacts with the NF-kappa B site of the human immunodeficiency virus enhancer. J Virol 63:2557-66.

67. Wang X, Hussain S, Wang EJ, Li MO, Garcia-Sastre A, Beg AA. 2007. Lack of essential role of NF-kappa B p50, RelA, and cRel subunits in virus-induced type 1 IFN expression. J Immunol 178:6770-6.

68. Wang J, Basagoudanavar SH, Wang X, Hopewell E, Albrecht R, Garcia-Sastre A, Balachandran S, Beg AA. 2010. NF-kappa B RelA subunit is crucial for early IFN-beta expression and resistance to RNA virus replication. J Immunol 185:1720-9.

69. Wang X, Wang J, Zheng H, Xie M, Hopewell EL, Albrecht RA, Nogusa S, Garcia-Sastre A, Balachandran S, Beg AA. 2014. Differential requirement for the IKKbeta/NF-kappaB signaling module in regulating TLR- versus RLR-induced type 1 IFN expression in dendritic cells. J Immunol 193:2538-45.

70. Jin J, Hu H, Li HS, Yu J, Xiao Y, Brittain GC, Zou Q, Cheng X, Mallette FA, Watowich SS, Sun SC. 2014. Noncanonical NF-kappaB pathway controls the production of type I interferons in antiviral innate immunity. Immunity 40:342-54.

71. Ruland J, Duncan GS, Wakeham A, Mak TW. 2003. Differential requirement for Malt1 in T and B cell antigen receptor signaling. Immunity 19:749-58.

72. Oetke C, Vinson MC, Jones C, Crocker PR. 2006. Sialoadhesin-deficient mice exhibit subtle changes in B- and T-cell populations and reduced immunoglobulin M levels. Mol Cell Biol 26:1549-57.

73. Jung S, Unutmaz D, Wong P, Sano G, De los Santos K, Sparwasser T, Wu S, Vuthoori S, Ko K, Zavala F, Pamer EG, Littman DR, Lang RA. 2002. In vivo depletion of CD11c+ dendritic cells abrogates priming of CD8+ T cells by exogenous cell-associated antigens. Immunity 17:211-20.

74. Miyake Y, Asano K, Kaise H, Uemura M, Nakayama M, Tanaka M. 2007. Critical role of macrophages in the marginal zone in the suppression of immune responses to apoptotic cell-associated antigens. J Clin Invest 117:2268-78.

75. Iwata A, Nishio K, Winn RK, Chi EY, Henderson WR, Jr., Harlan JM. 2003. A broad-spectrum caspase inhibitor attenuates allergic airway inflammation in murine asthma model. J Immunol 170:3386-91.

76. Hotchkiss RS, Chang KC, Swanson PE, Tinsley KW, Hui JJ, Klender P, Xanthoudakis S, Roy S, Black C, Grimm E, Aspiotis R, Han Y, Nicholson DW, Karl IE. 2000. Caspase inhibitors improve survival in sepsis: a critical role of the lymphocyte. Nature Immunology 1:496-501.

674 **Figure Legends**

675 **Fig. 1: Vesicular stomatitis virus infection leads to infiltration of TNF producing**
676 **phagocytes.**

677 **(A to F)** WT mice were infected with $2 \times 10^8$ PFU vesicular stomatitis virus (VSV). **(A)**
678 Tumor necrosis factor (TNF)-α mRNA expression levels in WT spleen tissue were
679 determined at the indicated time points after infection *(n=4-10)*. (**B**) Surface molecule
680 expression of CD11b, CD11c, CD8, and CD19 on $TNF^+$ cells is shown 4h after infection
681 (purple gate, whole spleen; pink gate, $TNF^+$ cells) (one representative result of n=5 is shown).
682 (**C**) Splenocytes from WT mice were stained for intracellular TNF production. $TNF^+CD11b^+$
683 cells were determined (as % of total $CD11b^+$ cells; n=5). **(D)** TNF-α mRNA expression was
684 determined in the spleen of WT, *Jh*$^{-/-}$, *Rag*$^{-/-}$, and *CD8*$^{-/-}$ mice 4 h after infection *(n=5-6)*. **(E)**
685 Surface molecule expression of TNF producing cells is shown 4h after infection. $CD3^-CD8^-$
686 $CD19^-NK1.1^-$ cells were further characterized for expression of CD11b, CD11c, Ly6C,
687 Ly6G, F4/80, MHC II, and CD115 on $TNF^+$ cells *(n=6)*. **(F)** $CD3^-CD8^-CD19^-NK1.1^-$
688 $CD11b^+Ly6C^+Ly6G^+TNF^+$ cells were quantified in spleen tissue 4h after infection *(n=6)*.
689 **(G**) Mice were injected with PBS-liposomes or clodronate- liposomes. Spleen tissue was
690 harvested after 24h. Sections from snap frozen spleen tissue were stained with anti-F4/80
691 antibodies (n=3). **(H)** TNF-α mRNA expression was determined in the spleen of WT,
692 clodronate-treated WT, *Ifnar*$^{-/-}$, DT-treated CD169-DTR, and CD11c-DTR mice 4 h after
693 infection *(n=6)*.

694

**Fig. 2: Tumor necrosis factor is required for early innate immune activation via maintenance of CD169$^{+}$ cells during viral infection.**

**(A to D)** Mice were infected with $10^5$ PFU VSV. **(A)** Survival of Wild-type (WT) and tumor necrosis factor-α null (*Tnfa*$^{-/-}$) mice was monitored for 20 days after infection (*n=9-12*). **(B)** Titers of neutralizing total immunoglobulin (Ig; left) and IgG (right) were determined in WT and *Tnfa*$^{-/-}$ mice at indicated time points after infection (*n=7*). **(C)** Interferon (IFN)-α and β concentrations were determined in the sera of WT and *Tnfa*$^{-/-}$ mice 24 h after infection (n=6-9). **(D)** IFN-α levels were determined in sera from WT and CD169-DTR mice 24 h after infection *(n=6).* **(E)** IFN-α and β concentration was determined in the sera of WT and *Tnfa*$^{-/-}$ mice injected with 200µg of polyinosinic:polycytidylic acid (polyI:C) at indicated time points *(n=3).* **(F)** WT and *Tnfa*$^{-/-}$ mice were infected with $2 \times 10^8$ plaque-forming units (PFU) of VSV. Snap-frozen spleen sections were stained with anti-CD169 antibodies (clone: MOMA-1) at indicated time points (one representative result of n=6 mice is shown; scale bar = 100 µm). **(G)** MFI of CD169 was quantified across spleen section from naïve and VSV infected WT and *Tnfa*$^{-/-}$ mice using ImageJ (1-3 images per spleen from 3-4 mice were analyzed). **(H)** MFI from *Tnfa*$^{-/-}$ mice was normalized to WT MFI **(I)** Snap-frozen spleen sections from WT and *Tnfa*$^{-/-}$ mice were stained for VSV glycoprotein (VSV-G) expression (clone: Vi10) after infection with $2 \times 10^8$ PFU VSV at indicated time points (one representative result of n=6 mice is shown; scale bar = 100µm). **(J)** MFI of VSV-G expression was quantified across spleen section from naïve and VSV infected WT and *Tnfa*$^{-/-}$ mice using ImageJ (1-3 images per spleen from 3-4 mice were analyzed) **(K)** WT and *Tnfa*$^{-/-}$ mice were infected with $10^5$ PFU VSV. Viral titers were measured in the spleen of WT and *Tnfa*$^{-/-}$ mice 8 h after infection with VSV (*n=6*). **(L)** *Tnfa* mRNA expression was determined

718 in spleen tissue of WT mice before and 4h after injection with UV-inactivated VSV *(n=4)*.
719 (M) Spleen tissue sections were stained with anti-CD169 antibodies in WT and *Tnfa*$^{-/-}$ mice
720 8h after infection with $2\times10^8$ PFU of ultraviolet (UV)-inactivated VSV (one representative
721 result of n=3 is shown). **(N)** Sections from snap-frozen spleen tissue harvested from WT and
722 *CD169*$^{-/-}$ mice were stained for CD169 and VSV-G 7h after infection with $2\times10^8$ PFU VSV
723 (n=3; scale bar = 100 µm).

724

725 **Fig. 3: VSV replication is sustained via TNFR1 on CD169$^+$ cells.**

726 **(A)** Spleen tissue sections from wild-type (WT), *Tnfrsf1a*$^{-/-}$ (tumor necrosis factor receptor 1
727 [TNFR1]), and *Tnfrsf1b*$^{-/-}$ (TNFR2) mice were stained with anti-CD169 and VSV-G
728 antibodies 8 h after infection with $2 \times 10^8$ PFU of VSV (One representative result of n=6
729 mice is shown; scale bar = 100µm). **(B)** MFI of CD169 was quantified across spleen sections
730 from WT, *Tnfrsf1a*$^{-/-}$, and *Tnfrsf1b*$^{-/-}$ infected mice, using ImageJ (1-3 images per spleen from
731 3-4 mice were analyzed). **(C-G)** WT, *Tnfrsf1a*$^{-/-}$, and *Tnfrsf1b*$^{-/-}$ mice were infected with $10^5$
732 PFU VSV. **(C)** Viral titers were measured in spleen tissue 8h after infection in WT, *Tnfrsf1a*$^{-/-}$,
733 and *Tnfrsf1b*$^{-/-}$ mice (*n=6-9*). **(D)** IFN-α concentration was determined in the sera of WT,
734 *Tnfrsf1a*$^{-/-}$, and *Tnfrsf1b*$^{-/-}$ mice 24 h after infection with VSV (*n=6-9*). **(E)** WT and *Tnfrsf1a*$^{-/-}$
735 mice were infected with $10^5$ PFU VSV. RNA expression levels of indicated genes were
736 determined in brain and spinal cord 24 h after infection (n=4-7, highest relative expression
737 values brain/spinal cord: *Eif2ak2*, 13.72/7.98; *Ifit2*, 5.41/6.13; *Ifit3*, 35.99/34.15; *Irf7*,
738 68.80/54.55; Isg15, 42.54/51.23; *Oasl1*, 70.43/84.94). **(F)** WT and *Tnfrsf1b*$^{-/-}$ mice were
739 infected with $10^5$ PFU VSV. RNA expression levels of indicated genes were determined in

brain and spinal cord 24h after infection (n=3-4, highest relative expression values brain/spinal cord: *Eif2ak,* 29.84/18.21*; Ifit2,* 7.99/10.24; *Ifit3,* 41.05/51.25*; Irf7,* 166.79/88.58; Isg15, 29.78/52.99; *Oasl1,* 75.60/114.39). **(G)** Viral titers were measured in brain and spinal cord tissue of WT and *Tnfrsf1a*$^{-/-}$ mice, once *Tnfrsf1a*$^{-/-}$ mice exhibited hind limb paralysis (*n=3*). **(H)** Survival of WT, *Tnfrsf1a*$^{-/-}$, and *Tnfrsf1b*$^{-/-}$ mice was monitored over time after infection with VSV (*n=15-24*).

**Fig. 4: TNFR1 on CD169$^{+}$ cells is essential for early IFN-I response.**

**(A)** Follicular B cells (CD19$^{+}$CD23$^{+}$) (FB), marginal zone B cells (CD19$^{+}$CD21$^{+}$ CD23$^{-}$) (MZB), and regulatory B cells (CD19$^{+}$CD21$^{+}$ CD5$^{+}$IgM$^{+}$) (RB) were analyzed in naïve WT, *Tnfa*$^{-/-}$, *Tnfrsf1a*$^{-/-}$, and *Tnfrsf1b*$^{-/-}$ deficient mice (*n=6*). **(B)** Lymphotoxin α (*LTα)*, *LTβ,* and lymphotoxin β receptor (*LtβR)* gene expression was determined in spleen tissue from WT and *Tnfrsf1a*$^{-/-}$ mice by reverse-transcription polymerase chain reaction (RT-PCR) (*n=3*). **(C)** Splenic B-cell populations FB, MZB, and RB were analyzed after infection with $2\times10^{8}$ PFU of VSV in WT and *Tnfrsf1a*$^{-/-}$ mice at indicated time points (*n=5*). **(D)** IFN-α concentration was determined 24 h after infection with $10^{5}$ PFU VSV in the sera of lethally irradiated mice reconstituted with either WT:*Rag*$^{-/-}$ or *Tnfrsf1a*$^{-/-}$:*Rag*$^{-/-}$ bone marrow at a ratio of 1:1 *(n=4).* **(E)** Neutralizing total immunoglobulin (Ig; left) and IgG (right) antibody titers were determined in the sera of WT:*Rag*$^{-/-}$ or *Tnfrsf1a*$^{-/-}$:*Rag*$^{-/-}$ reconstituted animals *(n=4)***. (F-H)** Lethally irradiated WT mice were reconstituted with bone marrow (BM) from WT or *Tnfrsf1a*$^{-/-}$ mice mixed with BM from **(F)** CD169-DTR and **(H)** CD11c-DTR at a 1:1 ratio. After 40 days, mice were infected with $10^{5}$ PFU of VSV. Before the infection mice were

762 treated with 2 doses of 100 ng DT via intra peritoneal injection **(F)** IFN-α concentration was
763 determined 24h after infection in the sera of WT:CD169-DTR and *Tnfrsf1a*$^{-/-}$:CD169-DTR
764 reconstituted animals *(n=4-5)*. **(G)** Neutralizing total immunoglobulin (Ig; left) and IgG
765 (right) antibody titers were determined in the sera of WT:CD169-DTR and *Tnfrsf1a*$^{-/-}$
766 :CD169-DTR reconstituted animals after infection with $10^5$ PFU VSV at indicated time
767 points (*n=4*). **(H)** IFN-α concentration was determined 24 h after infection in the sera of
768 WT:CD11c-DTR and *Tnfrsf1a*$^{-/-}$:CD11c-DTR reconstituted mice *(n=4-5)*.

769

770 **Fig. 5: Tumor necrosis factor mediates survival of CD169$^+$ cells via TNFR1**

771 **(A-E)** Mice were infected with $2 \times 10^8$ PFU VSV. **(A)** Caspase 3 activity was determined in
772 spleen tissue harvested from WT and *Tnfa*$^{-/-}$ mice 6h after infection with $2\times10^8$ PFU VSV
773 (n=4-7, RFU = relative fluorescence units). **(B)** *Bcl2*, *Bclxl*, *Xiap* RNA expression was
774 determined in spleen tissue from WT and *Tnfrsf1a*$^{-/-}$ mice 8h after infection (*n=3*). **(C)**
775 Tissue sections from WT and *Tnfa*$^{-/-}$ mice were stained with terminal deoxynucleotidyl
776 transferase dUTP nick end labeling (TUNEL) 5 h after infection *(*one result representative of
777 3 or 4 mice is shown; scale bar = 10 µm*)*. **(D)** Mean fluorescence intensity (MFI) of TUNEL
778 was quantified across spleen sections from naïve and VSV infected WT and *Tnfa*$^{-/-}$ mice
779 using ImageJ (1-2 images per spleen from 3-4 mice were analyzed). **(E)** At indicated time
780 points, the proportion of 7 aminoactinomycin D–positive (7AAD$^+$) cells among
781 CD11b$^+$CD169$^+$ cells were determined *(n=5)* in WT and *Tnfrsf1a*$^{-/-}$ mice. **(F)** WT, *Tnfa*$^{-/-}$ and
782 *Tnfrsf1a*$^{-/-}$ mice were treated with Z-Val-Ala-Asp-fluoromethylketone (zVAD-FMK) and
783 infected with $2 \times 10^8$ PFU VSV. Spleen tissue sections were stained with anti-CD169

antibodies 8 h after infection (one result representative of 3-4 mice is shown; scale bar = 100 µm). **(G)** MFI of CD169 was quantified across spleen sections from naïve and VSV infected WT and *Tnfa*$^{-/-}$ mice treated with Z-VAD using ImageJ (1-3 images per spleen from 3-4 mice were analyzed). **(H)** IFN-α concentration was determined 24 h after infection in the sera of Z-VAD treated WT and *Tnfa*$^{-/-}$ mice after infection with $10^5$ PFU of VSV (n=3).

**Fig. 6: VSV infection leads to TNFR1 dependent canonical NF-κB activation in splenic CD169$^+$ cells.**

**(A-D)** Sections of snap-frozen spleen tissue were harvested 4h after infection with 2 x $10^8$ PFU VSV. **(A)** Sections were stained for RelA before and after infection (one representative result of n=3 is shown; scale bar = 100 µm; side panel shows a cropped image; scale bar = 5 µm). **(B)** MFI of cytoplasmic and respective nuclear RelA was quantified in CD169$^+$ cells from WT mice before and after VSV infection to evaluate nuclear translocation of RelA (n = 48-63 are shown). **(C to E)** Spleen sections from WT and **(C)** *Tnfa*$^{-/-}$, **(D)** *Tnfrsf1a*$^{-/-}$ and **(E)** *Tnfrsf1b*$^{-/-}$ mice were stained with anti-RelA antibodies 4h after infection with $2\times10^8$ PFU VSV. MFI of RelA in the nucleus of CD169$^+$ was determined with ImageJ software (n=35-57).

**Fig. 7: MALT1 regulates translocation of RelA into the nucleus after infection with vesicular stomatitis virus.**

804 **(A)** Sections from snap-frozen spleen tissue harvested from naive *Malt1*$^{+/-}$ and *Malt1*$^{-/-}$ mice
805 were stained with anti-RelB antibodies (one representative result of n=3 is shown; scale bar =
806 10 µm). **(B)** MFI of cytoplasmic and nuclear RelB was quantified in CD169$^{+}$ cells using
807 ImageJ (n=39-42). **(C)** Sections of snap-frozen spleen tissue from *Malt1*$^{+/-}$ and *Malt1*$^{-/-}$ mice
808 were stained with anti-RelA antibodies 4h after infection with 2 x $10^8$ PFU VSV. The MFI in
809 the nucleus of CD169$^{+}$ cells was quantified (n=29-41). **(D+E)** *Malt1*$^{+/-}$ and *Malt1*$^{-/-}$ mouse
810 embryonic fibroblasts (MEFs) were stimulated with 100 ng/ml recombinant mouse tumor
811 necrosis factor (rmTNF) at indicated time points. Cytosolic (CE) and nuclear extracts (NE)
812 were harvested and probed for p65. Densitometry analysis of p65 and RelB was performed
813 on the WB images from cytosolic and nuclear fractions at indicated time points. Proteins
814 were normalized to GAPDH or histone (n=4).

815 **Fig. 8: MALT1 promotes vesicular stomatitis virus replication in CD169$^{+}$ cells and**
816 **immune activation during viral infection.**

817 **(A)** Spleen sections from naïve *Malt1*$^{+/-}$ and *Malt1*$^{-/-}$ mice were stained with anti-CD169 (one
818 representative result of n=3 is shown; scale bar = 100 µm). **(B)** Sections of snap-frozen
819 spleen tissue from *Malt1*$^{+/-}$ and *Malt1*$^{-/-}$ mice were analyzed 8h after infection with 2 x $10^8$
820 PFU VSV, stained with anti-CD169 and anti–vesicular stomatitis virus glycoprotein (VSV-
821 G) (one representative result of n=3 is shown; scale bar = 100 µm). **(C)** MFI of CD169 and
822 VSV-G was quantified across spleen sections from VSV infected *Malt1*$^{+/-}$ and *Malt1*$^{-/-}$ mice
823 using ImageJ (n=4). **(D and E)** Mice were infected with $10^5$ PFU VSV. **(D)** Viral titers were
824 measured in spleen tissue of *Malt1*$^{+/-}$ and *Malt1*$^{-/-}$ mice 8h after infection (*n=6*). **(E)** IFN-α
825 concentration was determined in the sera of *Malt1*$^{+/-}$ and *Malt1*$^{-/-}$ mice 24 h after infection
826 (*n=6*). **(F)** IFN-α concentration was determined in the sera of *Malt1*$^{+/-}$ and *Malt1*$^{-/-}$ mice

injected with 200µg polyinosinic:polycytidylic acid (poly I:C) at indicated time points *(n=3-4)*. **(G)** Survival of *Malt1*$^{+/-}$ and *Malt1*$^{-/-}$ animals was monitored for 20 days after infection (*n=13-14*).

**Fig. 1**

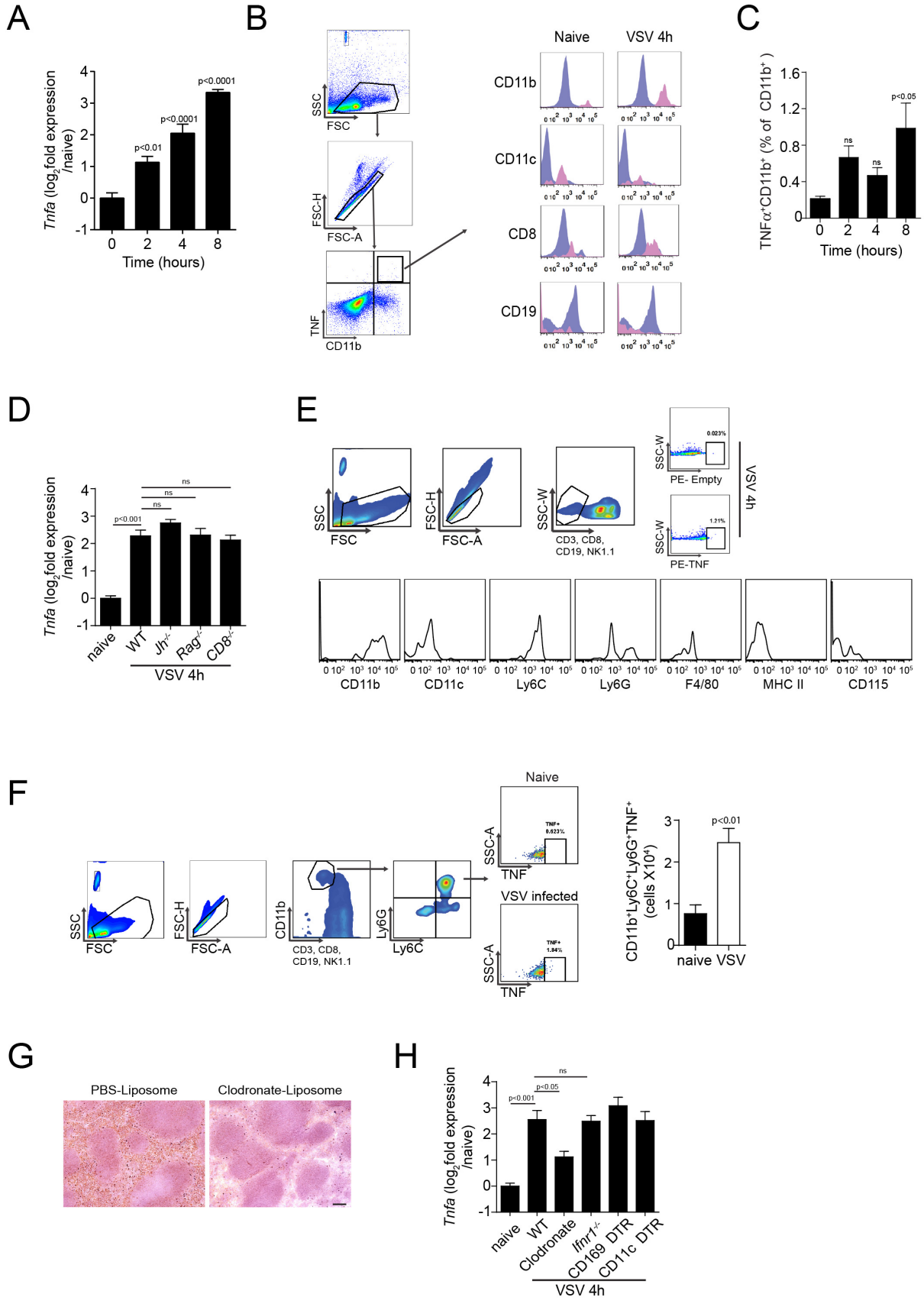

## Fig. 2

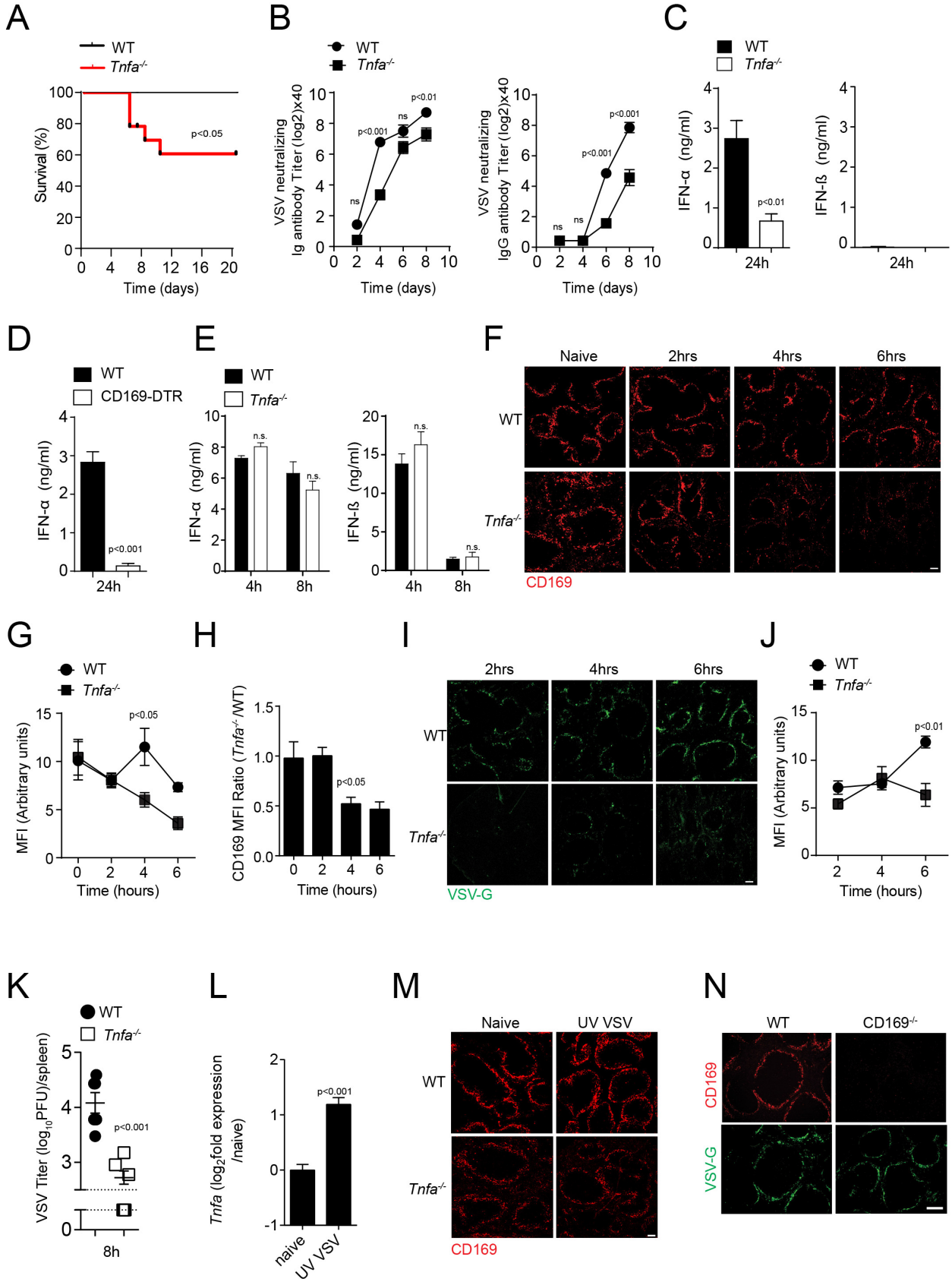

**Fig. 3**

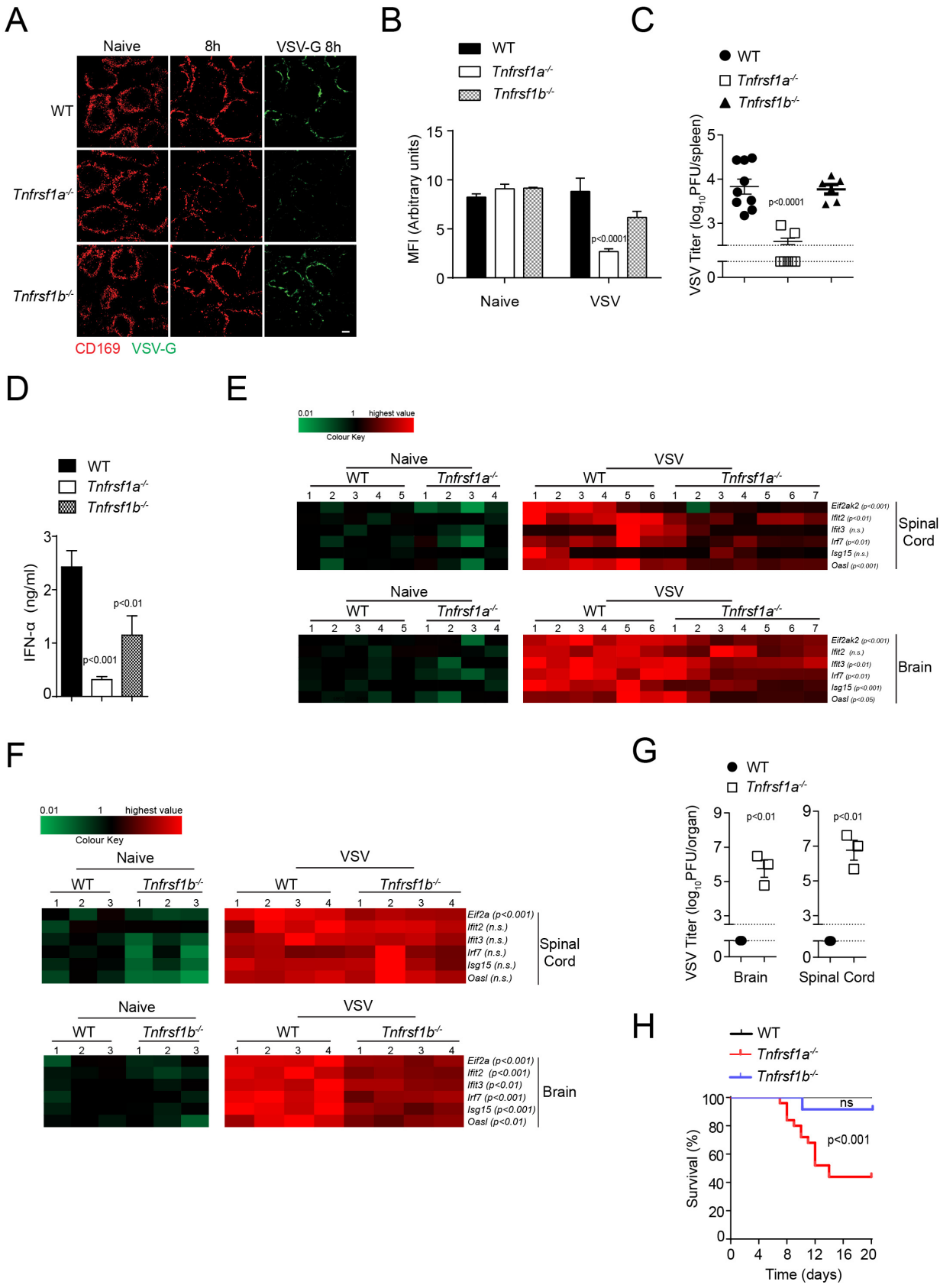

# Fig 4

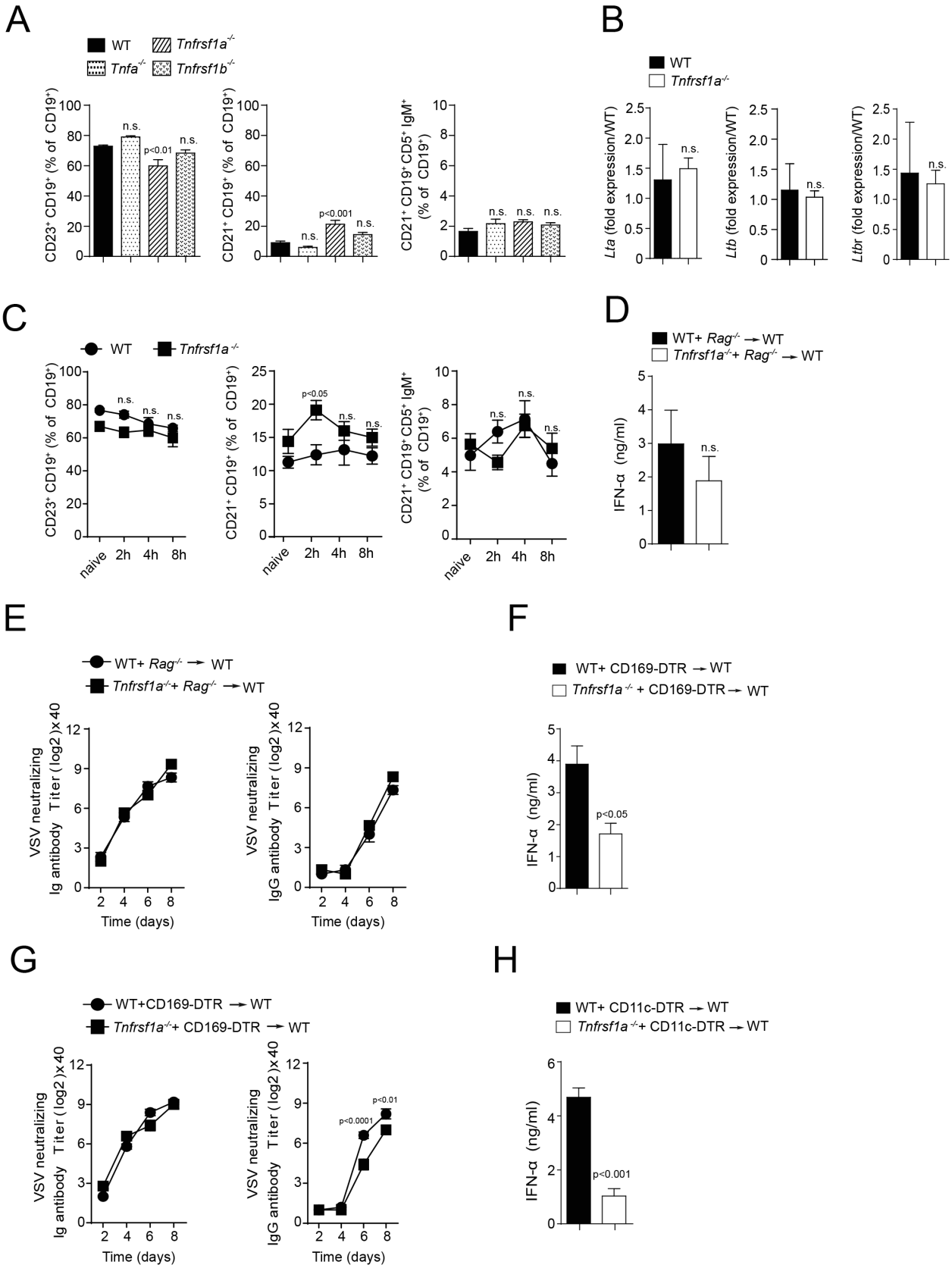

**Fig.5**

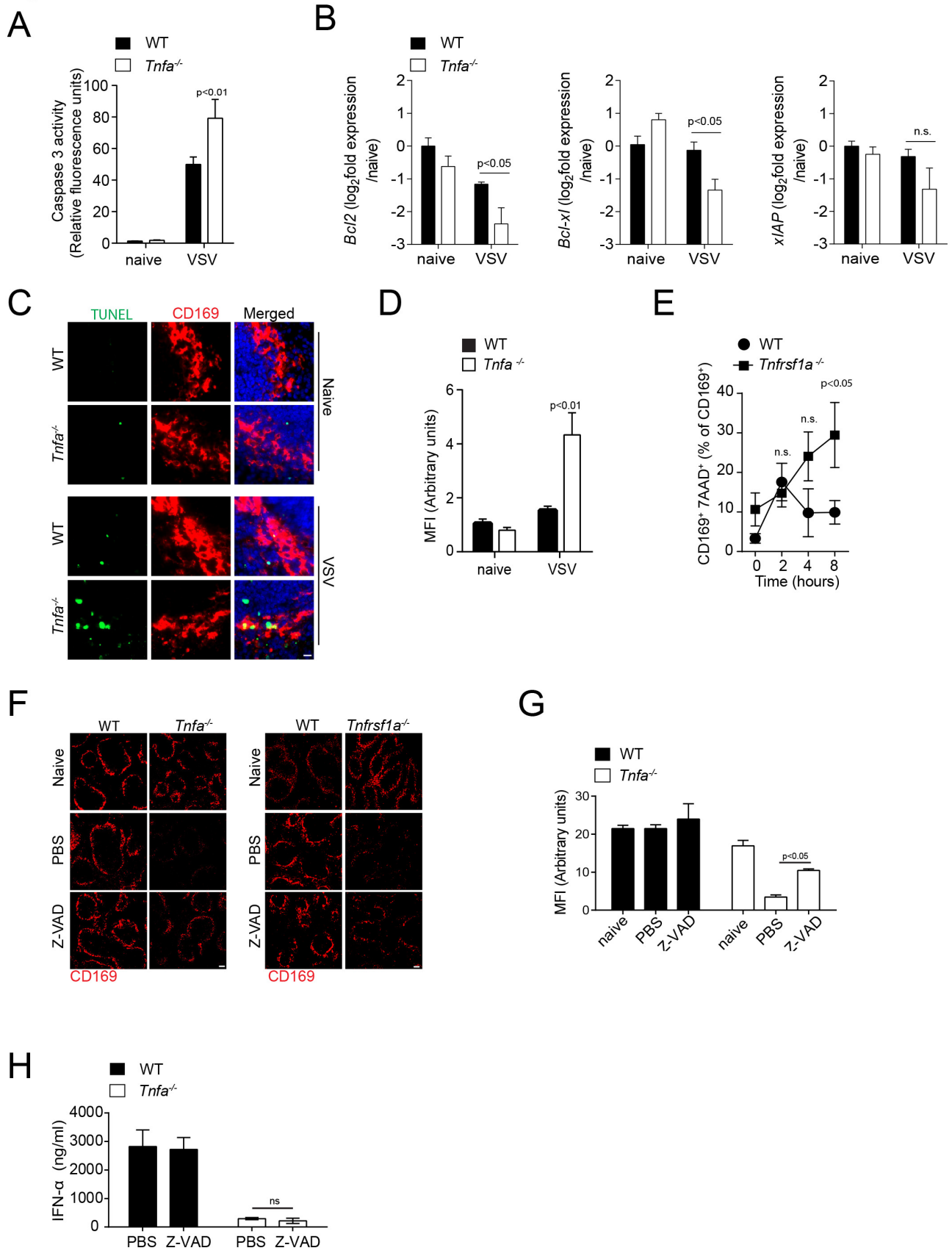

**Fig. 6**

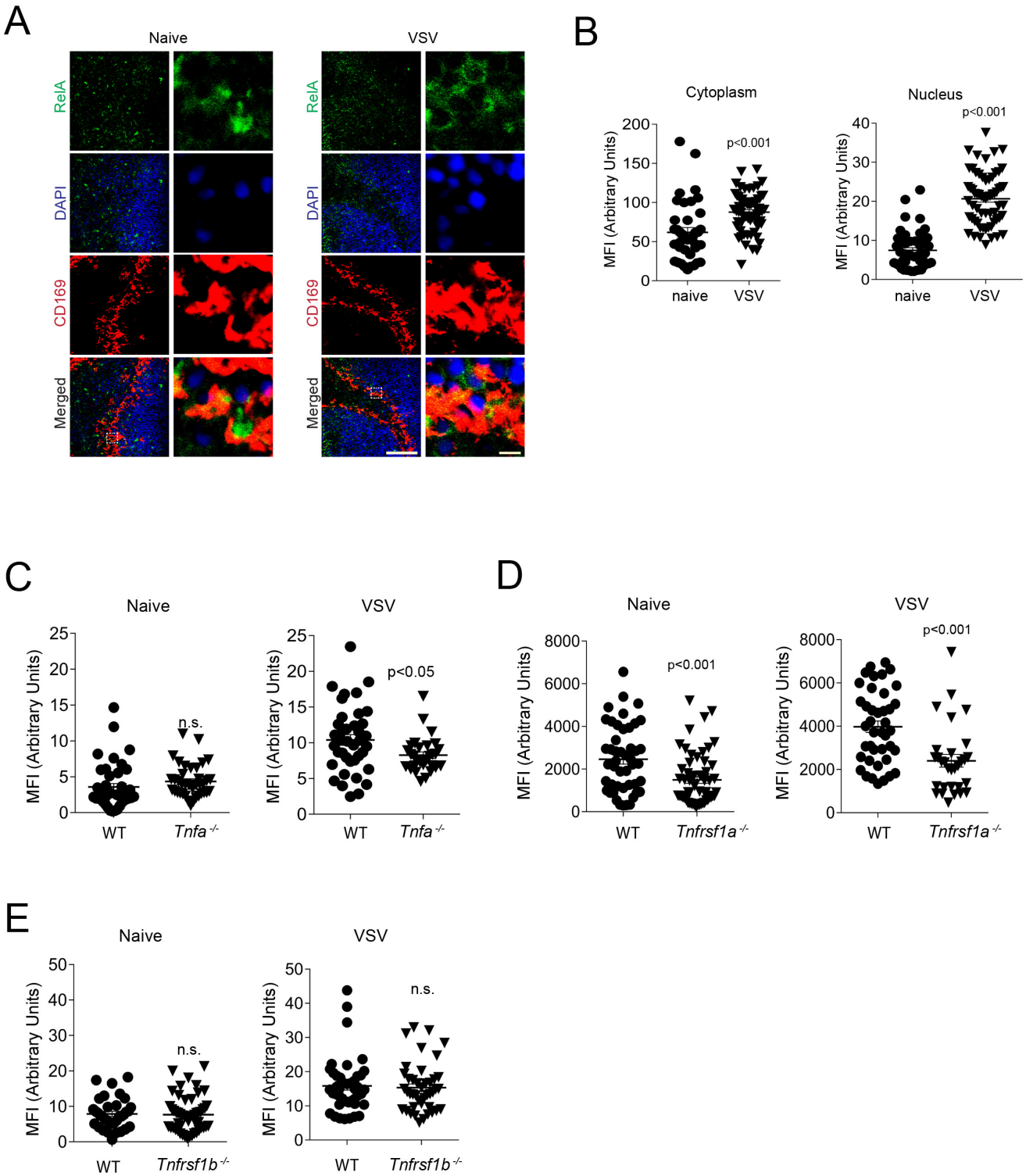

# Fig. 7

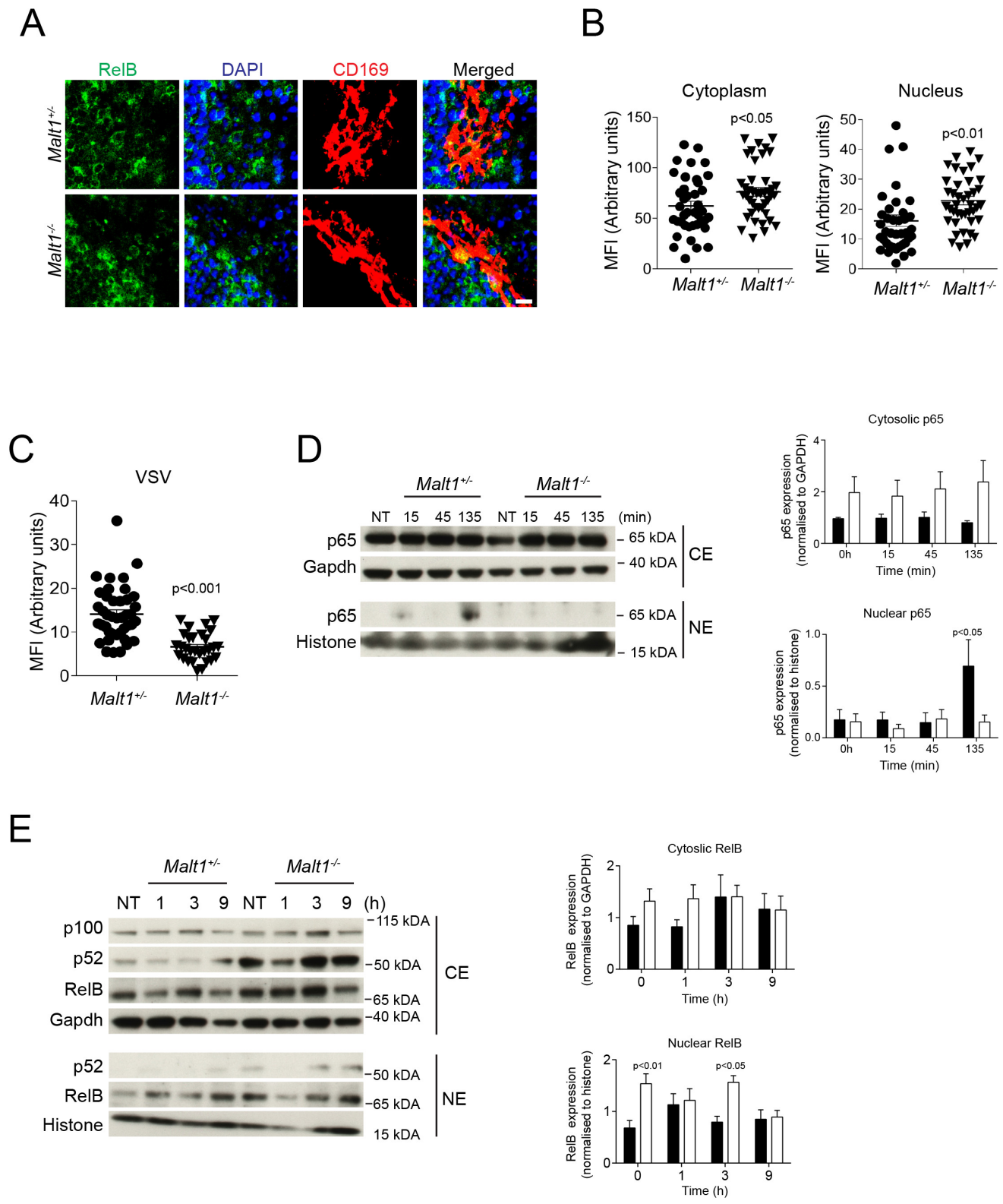

# Fig. 8